

Enhancing phosphorus availability in phosphorus-fertilized zones by reducing phosphate adsorbed on ferrihydrite using rice straw-derived biochar

Hao-Jie Cui · Ming Kuang Wang · Ming-Lai Fu · En Ci

Received: 30 May 2011 / Accepted: 19 July 2011 / Published online: 4 August 2011
© Springer-Verlag 2011

Abstract

Purpose Biochar amendments can alter phosphorus (P) availability in soils, though the influencing mechanisms are not yet fully understood. This work investigated the adsorption and desorption of P on ferrihydrite (F, a Fe-oxide widely distributed in surface environments) in order to evaluate the interactions between P and Fe-oxide in the absence or presence of biochar (F or ferrihydrite–biochar (F–B) interaction) in soils.

Materials and methods Biochar was produced by pyrolysis of rice straw at 600°C in steel ring furnaces. Two-line ferrihydrite was synthesized by dropwise addition of 1 mol L⁻¹ KOH into Fe(NO₃)₃ solution until the pH reached 7–8 while stirring vigorously. An F–B complex was prepared under similar conditions, except that a mixture of 10 g biochar and the Fe(NO₃)₃ solution was

used as the starting material instead of Fe(NO₃)₃ alone. A batch equilibration method was used to determine sorption or desorption of P. The mechanisms of P adsorption on F and F–B complex materials were discussed.

Results and discussion Adsorption of P on F decreased as the pH was increased from 3.0 to 10, but the adsorption capacity of F decreased by about 30–40% in the presence of biochar. The P chemisorption rates on F also decreased in the presence of biochar. The Freundlich model showed that the active adsorption sites on the surface of the F–B complex were energetically heterogeneous. The desorbability of adsorbed P on F was enhanced by combination with biochar. The mechanisms of P adsorption on F and F–B complex materials are different.

Conclusions The results showed that the amount and rate of P adsorption on the surface of ferrihydrite decreased with the presence of biochar, and the desorbability of adsorbed P on ferrihydrite can be enhanced when combined with biochar. Thus, the presence of biochar can decrease P adsorption on the Fe-oxides and enhance P availability in soils.

Responsible editor: Leo Condron

H.-J. Cui · M.-L. Fu (✉)
Key Laboratory of Urban Environment and Health,
Institute of Urban Environment, Chinese Academy of Sciences,
Xiamen 361021, People's Republic of China
e-mail: mlfu@iue.ac.cn

H.-J. Cui
State Key Laboratory of Soil and Sustainable Agriculture,
Institute of Soil Science, Chinese Academy of Sciences,
Nanjing 210008, People's Republic of China

M. K. Wang
Department of Agricultural Chemistry,
National Taiwan University,
No. 1, Sec. 4, Roosevelt Road,
Taipei 106, Taiwan

E. Ci
College of Resources and Environment, Southwest University,
Chongqing 400716, People's Republic of China

Keywords Adsorb · Biochar · Fe-oxide · Ferrihydrite · Phosphate

1 Introduction

Phosphorus (P) deficiency is one of the main factors restricting crop yields in many soils. Although P is naturally present at a high concentration in some soils worldwide, it is often a limiting nutrient in many other soils, in part due to strong adsorption on the surface of Fe (III)-(hydr)oxides in soils (Guzman et al. 1994; Jaisi et al. 2010; Johnson and Loeppert 2006). Ferrihydrite (F) is the

most effective Fe-oxide for phosphate (P) adsorption in soils due to its small particle size, high surface area, and high reactivity (Antelo et al. 2010). In nature, F is formed by the rapid oxidation of Fe(II) in Fe-rich waters, yielding an amorphous material (Rhoton et al. 2002), which occurs widely in surface environments such as soils and sediments. Hence, the adsorption of P on F has an important role in controlling transport, fate, and bioavailability of P in soils.

Biochar is a carbon-rich solid material produced by pyrolysis of biomass and can be added to soils as a means of abating climate change by sequestering carbon (Liu et al. 2011; Woolf et al. 2010), while also improving soil functions (Atkinson et al. 2010; Yuan et al. 2011). Biochar amendments can improve soil nutrient-holding capacity for crop production (Liang et al. 2006; Novak et al. 2009) and encourage a host of beneficial microorganisms (Kolb et al. 2009). Moreover, it has shown strong adsorption affinity for organic compounds and heavy metals (Cao et al. 2009; Chen and Yuan 2011; Lou et al. 2011; Namgay et al. 2010; Wang et al. 2010; Zheng et al. 2010).

Several studies have demonstrated enhanced P uptake in the presence of biochar (DeLuca et al. 2009; Novak et al. 2009). Biochar can alter P availability directly through its anion exchange capacity or by influencing the activity/availability of cations that interact with P (DeLuca et al. 2009). Biochar can also provide indirect effects on P availability and uptake through changes in the soil environment for microorganisms (Atkinson et al. 2010). It is well known that a layer of Fe-(hydr)oxide can be deposited or precipitated on part of the biochar after application of biochar to soils (Joseph et al. 2010). Although P adsorption characteristics of single-component Fe-(hydr)oxides have been widely studied (Arai and Sparks 2001; Jaisi et al. 2010; Khare et al. 2007), limited work has been conducted on the adsorption characteristics of the F–B complex to determine if it directly or indirectly influences the availability of P in soils. Therefore, the primary objective of this study was to investigate the P adsorption and desorption on F with and without biochar (F–B complex or F) and thereby evaluate the behavior of P in soils with added biochar.

2 Materials and methods

2.1 Materials

Biochar was produced by pyrolysis of rice straws obtained from a farm in Xiamen, China. It was air-dried for 1–2 days and then cut into pieces of approximately 2–3 cm in length. These pieces were pyrolyzed at 600°C in steel ring furnaces and sieved through a 1-mm screen to prepare biochar. Two-line ferrihydrite was synthesized as described by Schwertmann and

Cornell (2000). In a typical synthesis, 40 g of Fe (NO₃)₃·9H₂O was dissolved in 500 mL double-distilled water (DDW), and 330 mL of KOH (1 mol L⁻¹) was added to bring the pH to 7–8, while stirring vigorously. The solids were washed with DDW until free from electrolytes, and then freeze-dried. A ferrihydrite and biochar complex (F–B complex) was prepared under similar conditions, except that a mixture of 10 g biochar and the Fe(NO₃)₃ solution was used as the starting material instead of Fe(NO₃)₃ alone. All chemical reagents were analytical grade and purchased from Sinopharm Chemical Reagent Co., Ltd. (Shanghai, China) without further purification.

2.2 Characterization

The X-ray diffraction (XRD) patterns of the samples were analyzed with a Bruker D8 advance X-ray diffractometer equipped with a Cu K α radiation source operated at a tube voltage of 40 kV and a tube current of 40 mA. The data were collected in a step scan mode using steps of 0.02° with a scanning rate of 10° min⁻¹ in the 2 θ range from 5 to 90°. The morphology of F, biochar, and F–B complex materials was determined using a Hitachi S-4800 scanning electron microscope (SEM). The Fe concentration was determined using a scanning electron microscope coupled with an energy-dispersive X-ray spectrometer. A Micrometrics ASAP 2020M+C system was used to measure the surface areas and micropore size distributions of the materials. N₂ isothermal adsorption and desorption experiments were performed at relative pressures (P/P_0) from 10⁻⁶ to 0.9944 and from 0.9944 to 0.047, respectively. Pore size distribution was constructed by analyzing desorption data points using the BJH method. The point of zero charge (PZC) of the adsorbents was determined by a rapid potentiometric titration method (Cao et al. 2009, 2007). All Fourier transform infrared spectroscopy (FT-IR) spectra were obtained with a Thermo Scientific Nicolet iS10 spectrophotometer using pellets with KBr powder. Samples were scanned 15 times between 4,000 and 400 cm⁻¹ at a resolution of 4 cm⁻¹. Since FT-IR spectra subtraction was done at the slope of the absorption bands of the ferrihydrite (<1,100 cm⁻¹), it is difficult to preserve the P (ν_1) vibration modes at <800 cm⁻¹ if present. Therefore, the results discuss mainly changes in the P (ν_3) vibration modes (825–1,175 cm⁻¹).

2.3 Adsorption and desorption experiments

P adsorption capacities of F and F–B complex materials were evaluated by measuring the time-dependent concentrations of P and total P in a batch system. In the experiment examining the pH edge, 0.2 g of F or F–B complex was mixed with 100 mg L⁻¹ of KH₂PO₄ solution

(100 mL) at pHs of 3.0, 4.0, 5.0, 6.0, 7.0, 8.0, 9.0, and 10, monitored with a pH-stat (TIM865, Titration Manager, Radiometer Analyzer). The suspensions were agitated on a shaker at 250 rpm and 25°C for 24 h, after which 5 mL of the solutions was intermittently sampled and filtered through a 0.22- μm syringe filter.

For P adsorption, 0.2 g of F or F–B complex was mixed with 100 mg L⁻¹ of KH₂PO₄ solution (100 mL) at pH 4.5. At time zero and at selected time intervals thereafter, 5 mL of the suspensions was taken and filtered through a 0.22- μm syringe filter. To examine the effect of initial P concentration on the P adsorption by the F and F–B complex materials, 2.0 g L⁻¹ of F or F–B complex was contacted with 0, 0.2, 1, 2, 5, 10, 20, 50, 100, 200, and 300 mg L⁻¹ of KH₂PO₄ at pH 4.5. The suspensions were agitated on a shaker at 250 rpm and 25°C for 24 h, after which the suspensions were intermittently filtered through a 0.22- μm syringe filter, and the solids were collected for measurement of P desorption.

The desorption of P loaded on F or F–B complex samples was done using 0.01 mol L⁻¹ of KCl or citric acid as desorbing agents. The suspensions were agitated on a shaker at 250 rpm and 25°C for 24 h. At the end of the experiment, the suspensions were filtered through a 0.22- μm syringe filter.

The residual P concentration was measured by an ion chromatograph (Dionex ICS-3000). Batch experiments were conducted in three replicates, and the results reported are mean values of the experimental data.

3 Results and discussion

3.1 Characterization of the samples

The XRD pattern of ferrihydrite showed two broad reflection peaks (Schwertmann and Cornell 2000). Biochar and F–B complex materials of XRD patterns showed trace quartz contents (i.e., 3.34 and 4.26 Å). The SEM image showed that the synthesized F presented as an aggregation of the nanoparticles (Fig. 1a). The biochar consisted of irregular plates and particles with different size ranges, and the surface of the biochar was smooth (see Fig. 1b). F was mainly coated on the surface of the biochar in the F–B complex materials (see Fig. 1c), and aggregation of the coated F also can be found on the surface of the biochar (see Fig. 1d). The properties of different samples are listed in Table 1. Clearly, the PZC of the F–B complex (6.5) is lower than that of the F sample (8.3), but the Brunauer–Emmett–Teller (BET) surface area of the F–B complex (314 m² g⁻¹) is higher than that of the F sample (219 m² g⁻¹). In addition, the Fe content of the F sample (67%) was slightly higher than that of the F–B complex (60.5%).

3.2 pH edge affect on P adsorption

Earlier studies have shown that solution pH is an important parameter affecting adsorption of phosphate on Fe-oxides (Luengo et al. 2007; Zeng et al. 2004; Zhong et al. 2007). Figure 2 demonstrates that the adsorption of P depends mainly

Fig. 1 SEM images of **a** ferrihydrite, **b** biochar, **c** F–B complex, and **d** an enlarged detail of F–B complex materials (c)

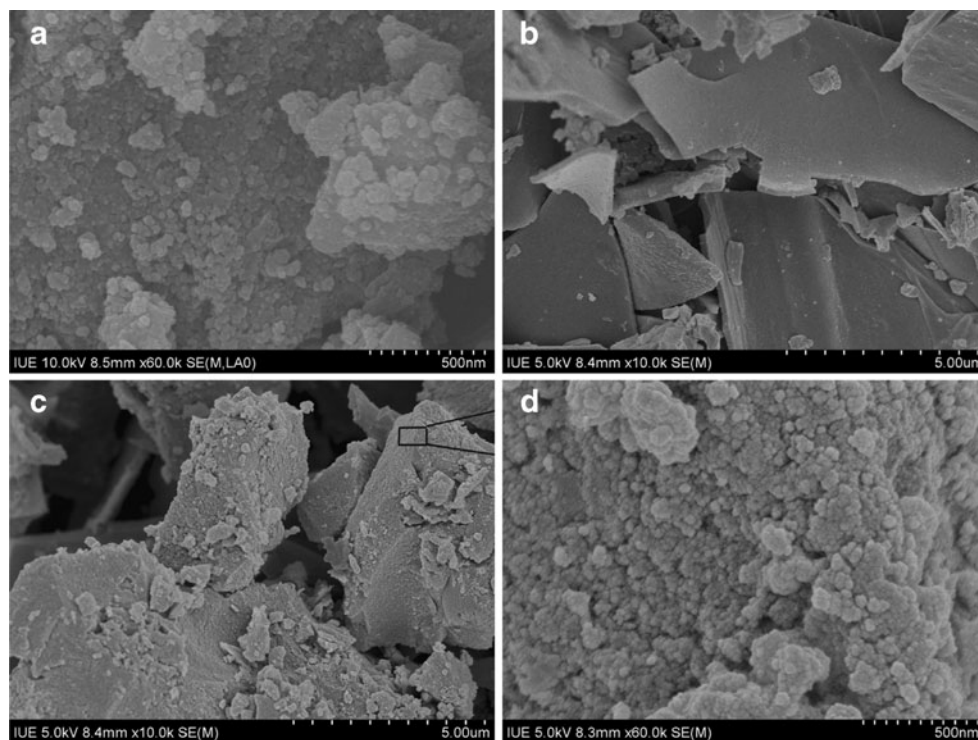


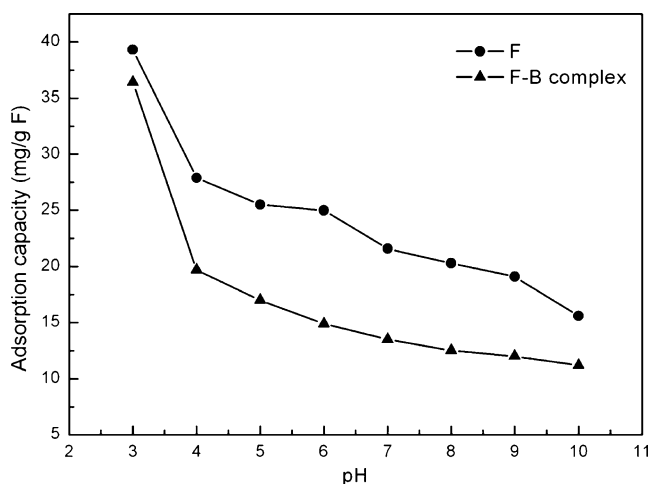
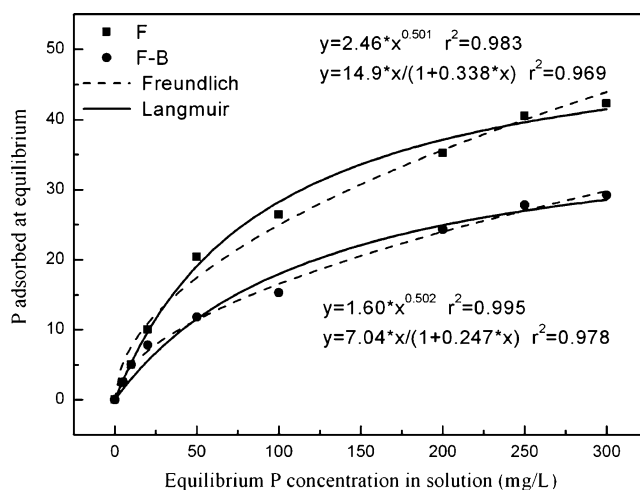
Table 1 Selected properties of adsorbents

Adsorbent	PZC	BET (m ² g ⁻¹)	Pore size (nm)	Fe (wt%)
Ferrihydrite (F)	8.3	219	3.3	67.0
Biochar (B)	1.9	39	17.1	0
F–B complex	6.5	314	3.9	60.5

on the pH of the aqueous solutions with the F and F–B complex materials, and the P adsorption decreases with increased solution pH, which can also be observed on the single-component Fe-(hydr)oxides (Arai and Sparks 2001). This is likely because the surface of the F nanoparticles bears more negative charge as the pH increases, causing a greater electrostatic repulsion toward the more negatively charged P forms (HPO₄²⁻ or PO₄³⁻) that predominate at the higher pH. Therefore, the lower adsorption of P at higher pH resulted from an increased repulsion force between the more negatively charged HPO₄²⁻ or PO₄³⁻ species and the negatively charged of the surface sites on F, and also because of increased OH⁻ ion competition. The single-component F in the absence of biochar (B) clearly shows higher adsorption ability than that of F combined with biochar materials (F–B complex). At a pH range from 4 to 10, the P adsorption capacity of F in the absence of biochar is about 30–40% higher than that of F combined with biochar (F–B complex). Thus, the presence of biochar decreased the adsorption of P on the surface of F. The decreased adsorption capacity of F can be attributed to the lower PZC of the F–B complex than that of F (see Table 1).

3.3 Adsorption isotherms

The amount of P adsorbed by the F and F–B complex increased with increasing initial P concentrations (Fig. 3).

**Fig. 2** Effect of pH on P adsorption at 25°C: adsorbent dose, 2 g L⁻¹; initial concentration, 100 mg L⁻¹ of KH₂PO₄ solution**Fig. 3** Equilibrium isotherm plots at 25°C. Solid and dashed lines represent the simulation using the Langmuir and Freundlich isotherm, respectively

In the low concentration region (<20 mg L⁻¹), the F and F–B complex materials are able to reduce the equilibrium P concentration to trace levels. At higher initial P concentrations, however, these F and F–B of two materials show different adsorption behaviors, with P adsorption capacity of F much higher than that of F–B complex.

Freundlich and Langmuir equations were fitted to the P adsorption data. The equations were as follows:

$$Q_e = K_f \times C_e^{1/n} \quad (1)$$

$$Q_e = b \times Q_m / (1 + b \times C_e) \quad (2)$$

where Q_e is the amount adsorbed per unit weight of sorbent at equilibrium (milligrams per gram), C_e is the equilibrium concentration (milligrams per liter), K_f is the Freundlich adsorption constant related to the P adsorption capacity of the adsorbent ((milligrams per gram)(liters per milligram)^{1/n}), and $1/n$ is the adsorption intensity, which indicates the favorability of adsorption. In addition, Q_m is the sorption capacity (milligrams per gram), and b is the affinity coefficient (liters per milligram). The Langmuir parameter Q_m is 44.2 mg g⁻¹ for F and 28.5 mg g⁻¹ for the F–B complex. The Freundlich model gave the higher r^2 values, showing that the adsorption of P onto F and F–B complex materials could be better described by the Freundlich model than by the Langmuir equation (see Fig. 3). These results indicated that the active adsorption sites were energetically heterogeneous and were not restricted to the formation of a monolayer.

3.4 Adsorption kinetics

Phosphate was rapidly adsorbed onto the F and F–B complex (Fig. 4). Nearly 80% of the P adsorption capacity

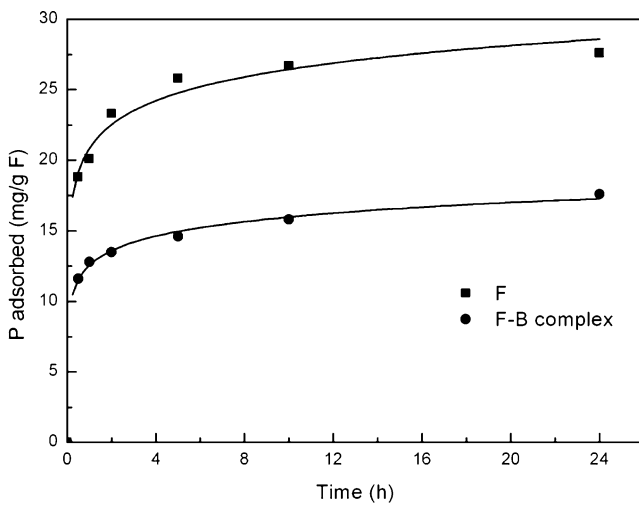


Fig. 4 Adsorption kinetics of P onto F and F–B complex materials: adsorbent dose, 2 g L⁻¹; P concentration, 100 mg L⁻¹; initial pH 4.5; temperature, 25°C

was reached within 2 h, and then, P adsorption increased steadily to reach equilibrium in about 24 h. This slow adsorption rate following an initially rapid adsorption of P has been observed previously (Jaisi et al. 2010). In order to investigate the mechanism of adsorption and potential rate-controlling steps, the pseudo-first-order, pseudo-second-order, and Elovich equation kinetic models have been employed to fit the experimental data, and the kinetic parameters for P adsorption are listed in Table 2. The calculated q_e values from the pseudo-first-order and pseudo-second-order linear plots did not agree well with the experimental ones, indicating that the adsorption of P onto F probably did not follow the pseudo-first-order and pseudo-second-order kinetic models. Compared with r^2 values, kinetics data for the adsorption of P from aqueous solution were in good agreement with the Elovich equation. The validity of the Elovich equation suggests that P adsorption on the F and F–B complex materials is a chemical adsorption

on highly heterogeneous adsorbents, and chemisorption mechanism is likely rate controlling in the processes (Chang and Juang 2005; Gupta and Bhattacharyya 2006). The α value of F is much higher than that of F–B complex materials (see Table 2), and the β shows the opposite trend, indicating that the initial rate of adsorption of F is faster than that of F–B complex materials. Thus, the rate of P chemisorption on F can be decreased with the presence of biochar (B).

3.5 Desorption studies

The rate of P desorption from the Fe-oxides is clearly dependent on the particular desorption conditions, which include concentrations of various cations in solution and the gradient of P concentration. The P desorbability can be defined as the ratio of the desorbed P to the total adsorbed P by the adsorbents. Therefore, the desorbability of P can be used to indicate the degree of P desorption from the adsorptive materials. For P desorption study, the adsorbed materials were treated with 0.01 mol L⁻¹ KCl or citric acid, and the data are presented in Fig. 5. The desorbability of adsorbed P on the F and F–B complex materials clearly increased with increasing initial equilibrium concentrations of P for all treatments. At low initial P adsorption level (≤ 50 mg L⁻¹), there was no detectable P released from the F and F–B complex materials by KCl. Previous studies have reported that P can be adsorbed to Fe-oxides with monodentate and bidentate surface complexes (Antelo et al. 2010; Arai and Sparks 2001; Parfitt and Atkinson 1976; Zhong et al. 2007). At relatively low P concentration (≤ 50 mg L⁻¹), the surface species are bidentate surface complexes, which are difficult to extract by KCl solution. A minor contribution of a monodentate surface complex can be formed at high initial P concentrations (100 and 200 mg L⁻¹), and they could be released by KCl solution (Khare et al. 2007; Liu et al. 1995). On the other hand,

Table 2 Kinetic parameters for P adsorption on F and F–B complex materials

Adsorbent	Pseudo-first-order ^a		Pseudo-second-order ^b		Elovich equation ^c		
	q_e (mg g ⁻¹ F)	r^2	q_e (mg g ⁻¹ F)	r^2	α [mg/(g min)]	β (g mg ⁻¹)	r^2
F	25.8	0.958	23.7	0.856	1.30×10^4	0.412	0.993
F–B complex	15.3	0.934	14.3	0.859	7.33×10^3	0.677	0.998

^a The kinetic model as proposed $\log(q_e - q_t) = \log q_e - k_1 \times t / 2.303$; q_e and q_t are the amounts of P adsorption (milligrams per gram) at equilibrium and at any instant of time t (minutes), respectively, and k_1 is the rate constant of pseudo-first-order adsorption (per minute)

^b The kinetic model as proposed $t/q_t = 1/(k_2 \times q_e^2) + t/q_e$; q_e and q_t are the amounts of P adsorption (milligrams per gram) at equilibrium and at any instant of time t (minutes), respectively, and k_2 is the equilibrium rate constant of pseudo-second-order adsorption (grams per milligram per minute)

^c The kinetic model as proposed $q_t - (1/\beta) \times \ln(\alpha \times \beta) + (1/\beta) \times \ln(t)$; q_t is the amount of adsorbed P at time t , α is the initial adsorption rate of the Elovich equation (milligrams per gram per minute), and β is the desorption constant related to the extent of surface coverage and activation energy for chemisorption (grams per milligram)

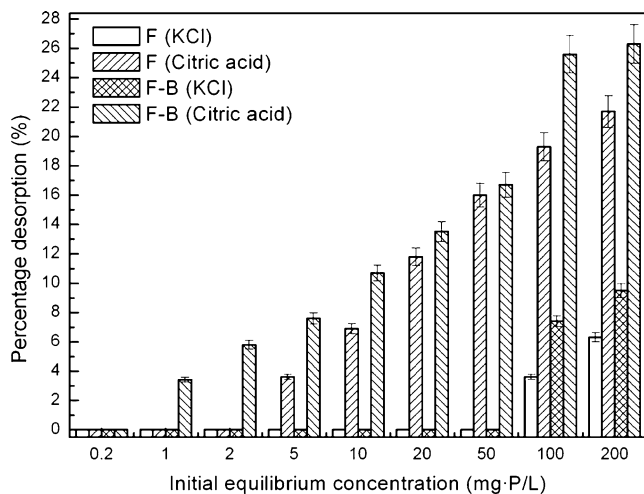


Fig. 5 Effect of initial equilibrium concentration on P desorption from F and F–B complex materials

there was also no detectable P released from the F and F–B complex by citrate acid with initial P equilibrium concentration at 0.2 mg L^{-1} . However, citrate acid released P from the F and F–B complex materials more effectively than KCl solution at higher initial P equilibrium concentration ($>0.2 \text{ mg L}^{-1}$), and ligand exchange should contribute to the greater extent to P release. The desorbability of adsorbed P on F–B complex is higher than that of F, indicating that the presence of biochar can enhance the desorbability of adsorbed P on F at higher initial P equilibrium concentration ($>0.2 \text{ mg L}^{-1}$).

3.6 Mechanism of P adsorption on F and F–B complex materials

Many researchers have investigated P adsorption mechanisms on Fe-oxides, and the monodentate, bidentate mononuclear, or bidentate binuclear surface complexes on F have been suggested by several researchers (Antelo et al. 2010; Arai and Sparks 2001; Jaisi et al. 2010; Khare et al. 2007). Figure 6a, b of the FT-IR spectra shows the loading level effects on the P surface complexes for F and F–B complex materials at pH 4.5. The broad spectrum with 5 mg g^{-1} loading level for F is an assemblage of three vibration bends (i.e., $1,083$; $1,034$; and 965 cm^{-1}), indicating these surface complexes are protonated bidentate complexes (Arai and Sparks 2001; Kwon and Kubicki 2004). As loading level increases, the FT-IR vibration mode at $1,037 \text{ cm}^{-1}$ becomes intensified (see Fig. 6a), indicating that diprotonated monodentate complexes are present at high loading level (Arai and Sparks 2001; Kwon and Kubicki 2004). By comparison, the broad FT-IR spectrum with 5 mg g^{-1} loading level for the F–B complex is also an assemblage of three vibration modes (i.e., $1,105$; $1,050$; and 977 cm^{-1}), and the loading level does not show to have a

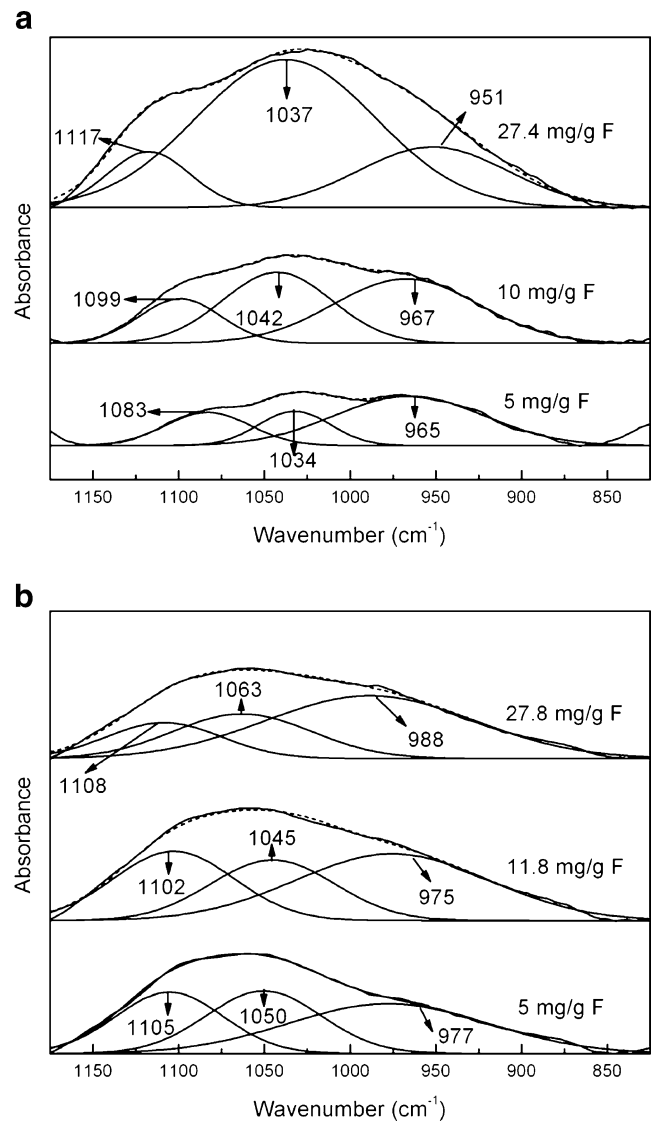


Fig. 6 FT-IR spectra of P adsorption complexes with different loading levels for pH 4.5 at the F–water interface: **a** F and **b** F–B complex

strong influence on the FT-IR spectra for the F–B complex (see Fig. 6b), suggesting that both diprotonated bidentate and diprotonated monodentate complexes can be formed on the surface of F–B complex. These differences can be attributed to the fact that the surface charge or function groups on the surface of ferrihydrite are altered by combining with biochar.

4 Conclusions

The adsorption and desorption of P on the surface of ferrihydrite combination with biochar were investigated to evaluate the influencing of biochar applications on interactions between P and Fe-oxide in soils. It was found that the P adsorption amount and adsorption rate on the surface

of F decreased with the presence of B, and the desorbability of adsorbed P on F can be enhanced when combined with B. Thus, the presence of B can decrease P adsorption on the Fe-oxides and enhance P availability in P-fertilized soils.

Acknowledgments The authors gratefully acknowledge the two anonymous reviewers for their helpful comments and improving the English. This project was supported by the Science Foundation from the State Key Laboratory of Soil and Sustainable Agriculture (Y052010028), the National Natural Science Foundation of China (41001139), the Start-Up Foundation from the Institute of Urban Environment, Chinese Academy of Sciences (Y0L5611B60), and the Natural Science Foundation Project of CQ CSTC (CSTC, 2009BB1108).

References

- Antelo J, Fiol S, Pérez C, Mariño S, Arce F, Gondar D, López R (2010) Analysis of phosphate adsorption onto ferrihydrite using the CD-MUSIC model. *J Colloid Interf Sci* 347:112–119
- Arai Y, Sparks DL (2001) ATR-FTIR spectroscopic investigation on phosphate adsorption mechanisms at the ferrihydrite-water interface. *J Colloid Interf Sci* 241:317–326
- Atkinson CJ, Fitzgerald JD, Hipps NA (2010) Potential mechanisms for achieving agricultural benefits from biochar application to temperate soils: a review. *Plant Soil* 337:1–18
- Cao X, Ma L, Gao B, Harris W (2009) Dairy-manure derived biochar effectively sorbs lead and atrazine. *Environ Sci Technol* 43:3285–3291
- Chang MY, Juang RS (2005) Equilibrium and kinetic studies on the adsorption of surfactant, organic acids and dyes from water onto natural biopolymers. *J Colloids Surf A: Physicochem Eng Aspects* 269:35–46
- Chen B, Yuan M (2011) Enhanced sorption of polycyclic aromatic hydrocarbons by soil amended with biochar. *J Soils Sediments* 11:62–71
- DeLuca TH, MacKenzie MD, Gundale MJ (2009) Biochar effects on soil nutrient transformation. Chapter 14. In: Lehmann J, Joseph S (eds) *Biochar for environmental management science and technology*. Earthscan, London, pp 251–280
- Feng XH, Zhai LM, Tan WF, Liu F, He JZ (2007) Adsorption and redox reactions of heavy metals on synthesized Mn oxide minerals. *Environ Pollut* 147:366–373
- Gupta SS, Bhattacharyya KG (2006) Adsorption of Ni(II) on clays. *J Colloid Interf Sci* 295:21–32
- Guzman G, Alcantara E, Barron V, Torrent J (1994) Phytoavailability of phosphate adsorbed on ferrihydrite, hematite, and goethite. *Plant Soil* 159:219–225
- Jaisi DP, Blake RE, Kukkadapu RK (2010) Fractionation of oxygen isotopes in phosphate during its interactions with iron oxides. *Geochim Cosmochim Acta* 74:1309–1319
- Johnson SE, Loeppert RH (2006) Role of organic acids in phosphate mobilization from iron oxide. *Soil Sci Soc Am J* 70:222–234
- Joseph SD, Camps-Arbestain M, Lin Y, Munroe P, Chia CH, Hook J, Zwieter L, Kimber S, Cowie A, Singh BP, Lehmann J, Foidl N (2010) An investigation into the reactions of biochar in soil. *Aust J Soil Res* 48:501–515
- Khare N, Martin JD, Hesterberg D (2007) Phosphate bonding configuration on ferrihydrite based on molecular orbital calculations and XANES fingerprinting. *Geochim Cosmochim Acta* 71:4405–4415
- Kolb SE, Fermanich KJ, Dombush ME (2009) Effect of charcoal quantity on microbial biomass and activity in temperate soils. *Soil Sci Soc Am J* 73:1173–1181
- Kwon KD, Kubicki JD (2004) Molecular orbital theory study on surface complex structures of phosphates to iron hydroxides: calculation of vibrational frequencies and adsorption energies. *Langmuir* 20:9249–9254
- Liang B, Lehmann J, Solomon D, Kinyangi J, Grossman J, O'Neill B, Skjemstad JO, Thies J, Luizão FJ, Petersen J, Neves EG (2006) Black carbon increases cation exchange capacity in soils. *Soil Sci Soc Am J* 70:1719–1730
- Liu F, He J, Li X, Xu F, He H, Wang D (1995) Chemical states of phosphorus adsorbed on goethite at various phosphate concentrations. *Chinese Sci Bull* 40:506–511
- Liu Y, Yang M, Wu Y, Wang H, Chen Y, Wu W (2011) Reducing CH₄ and CO₂ emissions from waterlogged paddy soil with biochar. *J Soils Sediments*. doi:10.1007/s11368-011-0376-x
- Lou L, Wu B, Wang L, Luo L, Xu X, Hou J, Xun B, Hu B, Chen Y (2011) Sorption and ecotoxicity of pentachlorophenol polluted sediment amended with rice-straw derived biochar. *Biores Technol* 102:4036–4041
- Luengo C, Brigante M, Avena M (2007) Adsorption kinetics of phosphate and arsenate on goethite. A comparative study. *J Colloid Interf Sci* 311:354–360
- Namgay T, Singh B, Singh BP (2010) Influence of biochar application to soil on the availability of As, Cd, Cu, Pb, and Zn to maize (*Zea mays* L.). *Aust J Soil Res* 48:638–647
- Novak JM, Busscher WJ, Laird DL, Ahmedna M, Watts DW, Niandou AS (2009) Impact of biochar amendment on fertility of a southeastern coastal plain soil. *Soil Sci* 174:105–112
- Parfitt RL, Atkinson RJ (1976) Phosphate adsorption on goethite (α -FeOOH). *Nature* 264:740–742
- Rhoton FE, Bigham JM, Lindbo DL (2002) Properties of iron oxides in streams draining the Loess Uplands of Mississippi. *Appl Geochem* 17:409–419
- Schwertmann U, Cornell RM (2000) *Iron oxides in the laboratory: Preparation and characterization*. Weinheim, Wiley-VCH Verlag GmbH
- Wang H, Lin K, Hou Z, Richardson B, Gan J (2010) Sorption of the herbicide terbuthylazine in two New Zealand forest soils amended with biosolids and biochars. *J Soils Sediments* 10:283–289
- Woolf D, Amonette JE, Street-Perrott FA, Lehmann J, Joseph S (2010) Sustainable biochar to mitigate global climate change. *Nature Commun* 1:1–9
- Yuan JH, Xu RK, Qian W, Wang RH (2011) Comparison of the ameliorating effects on an acidic ultisol between four crop straws and their biochars. *J Soils Sediments*. doi:10.1007/s11368-011-0365-0
- Zeng L, Li X, Liu J (2004) Adsorptive removal of phosphate from aqueous solutions using iron oxide tailings. *Water Res* 38:1318–1326
- Zheng W, Guo M, Chow T, Bennett DN, Rajagopalan N (2010) Sorption properties of greenwaste biochar for two triazine pesticides. *J Hazard Mater* 181:121–126
- Zhong B, Stanforth R, Wu S, Chen JP (2007) Proton interaction in phosphate adsorption onto goethite. *J Colloid Interf Sci* 308:40–48